

Importance of van der Waals interactions in hydrogen adsorption on a silicon-carbide nanotube revisited with vdW-DFT and quantum Monte Carlo

Genki I. Prayogo¹

School of Information Science, JAIST

Hyeondeok Shin

Computational Science Division, Argonne National Laboratory, Argonne, Illinois 60439, USA

Anouar Benali

Computational Science Division, Argonne National Laboratory, Argonne, Illinois 60439, USA

Ryo Maezono

School of Information Science, JAIST

Kenta Hongo

Research Center for Advanced Computing Infrastructure, JAIST

Abstract

DFT is a valuable tool for calculating adsorption energies toward designing materials for hydrogen storage. However, dispersion forces being absent from the theory, it remains unclear how the consideration of van der Waals (vdW) interactions affects such calculations. For the first time, we applied diffusion Monte Carlo (DMC) to evaluate the adsorption characteristics of a hydrogen molecule on a (5,5) armchair silicon-carbide nanotube (H₂-SiCNT). Within the framework of density functional theory (DFT), we also benchmarked various exchange-correlation functionals, including those recently developed for treating dispersion or vdW interactions. We found that the vdW-corrected DFT methods agree well with DMC, whereas the local (semilocal) functional significantly over (under)-binds. Furthermore, we fully optimized the H₂-SiCNT geometry within the DFT framework and investigated the correlation between structure and charge density. The vdW contribution to adsorption was found to be non-negligible at approximately 1 kcal/mol per hydrogen molecule, which amounts to 9–29 % of the ideal adsorption energy required for hydrogen storage applications.

Keywords: Hydrogen storage, Physisorption, van der Waals (vdW), vdW-DFT, Diffusion Monte Carlo, *ab initio*

1. Introduction

Hydrogen energy is a promising energy resource for reducing greenhouse gas emissions [1, 2, 3]. To realize the industrial use of hydrogen energy, particularly in the transportation sector, one of the most important developmental challenges is addressing the related storage issues—safety and capacity [2]. Several materials-based strategies to store hydrogen have been proposed, which involve choices such as the form of the stored hydrogen (physical vs. chemical storage) and the structure of the storage material (e.g., nanostructures and metal hydrides). To achieve adsorption-based room-temperature storage, the ideal interaction energy between the stored hydrogen and storage material has been estimated as approximately 3.5–11.5 kcal/mol [4, 5]. At the moment, this technology is limited to low-temperature storage because the interaction is too weak to resist being overpowered by thermal energy at

the desired higher temperatures. Computational materials design would be immensely helpful in further exploring appropriate storage materials from the massive materials space, provided the hydrogen adsorption energies on candidate materials can be accurately predicted at reasonable computational costs.

Silicon-carbide nanotubes (SiCNTs) are a typical nanostructure studied for the above purpose [6, 7, 8, 9] owing to their enhanced molecular interactions compared with that of the structurally related (and more common) carbon nanotubes. This feature has been linked to the SiCNT polarized surface originating from the Si–C bonds [10, 11, 12, 13]. Despite this, studies have suggested that in the pristine state, the adsorption energy of hydrogen on SiCNTs still lies below the required values, ranging between 0.7 and 1.98 kcal/mol. This has motivated further investigations into doping schemes with dopants such as al-

kali and transition metals [8, 14] or with vacancies [7, 15]. These studies, however, did not incorporate van der Waals (vdW) corrections into the conventional DFT scheme, and thus they may have underestimated the true adsorption potential. From another viewpoint, the basis sets adopted for DFT calculations also matter, since Gaussian and numerical basis sets can give rise to overestimated interaction energies owing to the basis set superposition error [16]. Thus, the true adsorption potential of SiCNTs remains unclear, even when the results seem plausible and are consistent with the experimentally observed higher hydrogen uptake than that of CNTs [17, 18].

In this study, we demonstrate the importance of incorporating vdW interactions for a quantitative description of H_2 adsorption on SiCNTs and related systems. To reproduce the vdW interactions accurately, we applied diffusion Monte Carlo (DMC) to evaluate the adsorption energy, which can serve as an accurate reference value. DMC has been proved to be highly accurate for various noncovalent systems [19, 20, 21, 22, 23, 24, 25, 26, 27, 28, 29] and is comparable to the best correlated methods while offering a better computational cost and minimal systematic error [27]. We then benchmarked several available vdW-DFT approaches by comparing them with DMC as well as conventional exchange-correlation (XC) functionals in terms of binding curves and charge densities to further investigate H_2 -SiCNT-related systems. Finally, we investigated the fully optimized H_2 -SiCNT geometries for our benchmark set of XC functionals and discussed their relationship to the charge densities at a fixed geometry, along with the implications of their difference in terms of the DMC charge densities.

2. Computational details

2.1. Structural modeling

We selected the type-I (5,5) armchair SiCNT with 20 atoms per primitive cell. Consisting only of Si-C bonds, type-I was found to be more stable than those containing Si-Si and C-C bonds [11, 30, 31]. The basic structure was built using a generic nanotube generation tool [32] and later optimized in DFT. A $14 \times 14 \times a$ Å simulation cell was used to minimize spurious interactions with periodic images, and the periodic unit length (a) was optimized along with the other geometries. We placed a hydrogen molecule with a fixed vertical orientation over an SiCNT hollow site (Figure 1). The distance was varied to obtain a binding curve, for which the energies were least-square-fitted to a Morse potential. The binding energy corresponding to the energy change from the free to the bound configuration is defined as

$$\Delta E(r) = E_{H_2-SiCNT}(r) - E_{H_2} - E_{SiCNT}. \quad (1)$$

Each component on the right-hand side was computed independently using the same simulation cell. Since the diameter of the SiCNT is not singular due to lengthwise

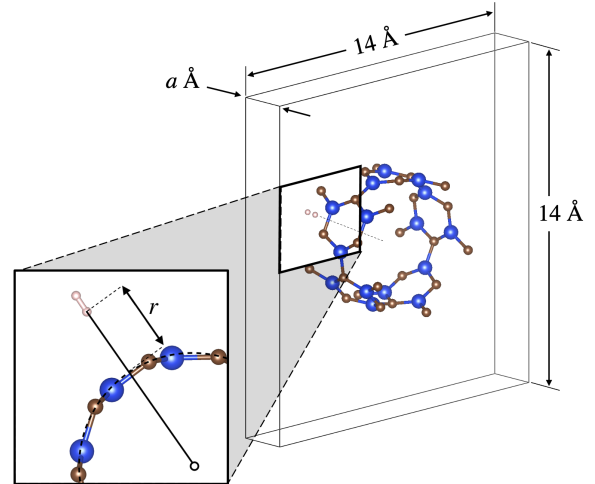


Figure 1: A vertically oriented hydrogen molecule over an SiCNT hollow site. Inset: the distance is measured over the largest diameter of the SiCNT, which corresponds to the C site.

buckling, we defined r as the distance from the hydrogen molecule to the center of the nanotube subtracted by the largest diameter within the primitive cell.

2.2. Density Functional Theory (DFT)

The PWSCF binary in the QUANTUM ESPRESSO [33] package was used for all DFT calculations based on plane wave basis sets with pseudopotentials. The kinetic energy cutoff and k-point grid size were converged at 150 hartree and a $1 \times 1 \times 6$ Monkhorst-Pack grid [34], respectively, to achieve chemical accuracy. To reduce the time-step error in the later DMC stage, the nonsingular energy-consistent pseudopotential reported by Burkatzki, Filippi, and Dolg [35] was utilized for all calculations. All geometry optimizations were performed within PBE with total force and energy thresholds of 10^{-10} and 10^{-4} a.u., respectively.

We compared the vdW approaches DFT-D2, DFT-D3, vdW-DF2, and rVV10 [36, 37, 38, 39, 40, 41], of which the first two are based on an explicit R^{-6} pairwise potential operating on atomic coordinates, whereas the latter have an exchange-correlation potential modified by the addition of a nonlocal correlation term. The additional term in the exchange-correlation potential allows for changes in the charge density, providing more information for analyzing the binding formation. The local density functional PZ [42] and gradient-corrected PBE [43] were employed as baselines.

2.3. Diffusion Monte Carlo (DMC)

QMCPACK [44] was used for all quantum Monte Carlo (QMC) calculations, the main DMC calculations, and for the variational Monte Carlo (VMC) calculations used in preparation of the trial wave function. The trial wave

function was a Slater–Jastrow type comprising a single determinant with PBE-DFT orbitals and a Jastrow factor with optimized parameters at the VMC level. Parameters consisting of one- and two-body interaction terms were used, each in the form of B-splines with 10 optimizable parameters for each atom type. For efficiency, Jastrow parameters were optimized using a hybrid method mixing the linear method algorithm [45] and an accelerated descent method as described by Otis and Neuscamann [46]; The orbitals were pre-projected into B-splines [47] to increase the computational efficiency. The pseudopotential parts were evaluated with the T -move scheme [48]. The time-step and finite size errors were eliminated through linear extrapolation, first by the time-step and then by the real space supercell size. The DMC time-steps were 0.0025, 0.01, and 0.04 a.u., and the supercells were 2, 6, and 8 times duplicates of the primitive unit cell in the cylinder length, each with twist-averaged boundary conditions [49] on regular grids of $1 \times 1 \times 8$, $1 \times 1 \times 3$, and $1 \times 1 \times 2$, respectively. The mixed boundary condition was applied with open boundaries on the 14 Å sides, and the target walker population was set to 4,096.

3. Results and Discussion

3.1. Structural properties

We found that the geometry of the (5,5) SiCNT is relatively unaffected by the choice of XC functional. (Table 1). This result is unsurprising due to its construction of only single covalent bonds involving s and p electrons. The obtained bond lengths were also consistent with those reported in prior hybrid works [30, 50], albeit slightly shorter than those obtained utilizing cluster models [8, 31]. It is not unusual to have a slight distortion near cluster terminations that does not exist in periodic models such as the one used in this work. Thus, we conclude that the conventional XCs are sufficient to describe the SiCNT model used in this work.

Table 1: LDA- and GGA-optimized structural parameters of a (5,5) SiCNT given in Å. The subscript d denotes diagonal bonds relative to the cylinder axis.

XC	R_{SiCNT}	Buckling	$\langle \text{Si-C} \rangle$	$\langle \text{Si-C}_p \rangle$	$\langle \text{Si-C}_d \rangle$
LDA	4.341	0.103	1.791	1.790	1.793
GGA	4.338	0.101	1.790	1.788	1.792

3.2. H_2 adsorption on SiCNT

The main interest is how well the adsorption curves from the vdW corrections agree with the DMC results and among themselves. As shown in Figure 2, it is clear that LDA (GGA) severely over (under)-binds the DMC target value by 25 (51) meV, or 0.6 (1.2) kcal/mol. This result is consistent with the established behavior of LDA and GGA in vdW-dominated systems. The non-empirical vdW-DF2

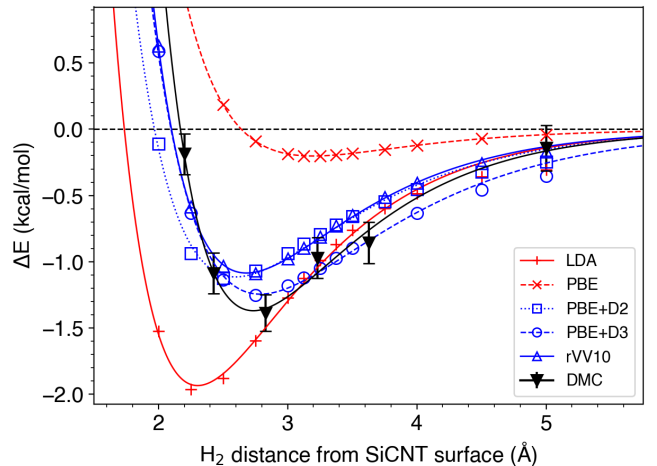


Figure 2: Binding energy curves of H_2 on an SiCNT with evaluated XCs and DMC. Colored dashes indicate each curve’s minimum. While energetically similar, the minima from the vdW-corrected XCs are at different locations, and they slightly underbind relative to DMC.

and rVV10 functionals return virtually identical binding energies, but their H_2 separations differ by approximately 0.2 Å. Interestingly, the D2 energetics agree more with the non-empirical methods relative to D3. This was accompanied by a slight underestimation of the H_2 separation distance, which was corrected by D3. Considering they both start from PBE energies, this is satisfactory. In general, all vdW corrections underbind relative to DMC but with more reasonable adsorption minima. This suggests that while the geometries derived from these functionals can generally be trusted, a more careful consideration of their energetics is necessary.

LDA is known to produce spurious covalent bonding between noncovalent molecules due to the self-interaction error [20, 24]. This gives rise to ca. 0.6 kcal/mol overbinding. GGA improves the self-interaction error, but at the cost of weak intermolecular interactions as the vdW interaction is not inherently accounted for. To illustrate this point, we plotted the charge density difference between the whole and isolated components, $\Delta\rho(r) = \rho_{\text{SiCNT}+\text{H}_2}(r) - \rho_{\text{SiCNT}}(r) - \rho_{\text{H}_2}(r)$, in Figure 3. The charge accumulation between the H_2 molecule and SiCNT, i.e., spurious covalent bonding, is prominent for LDA as shown in Fig. 3 (a). This feature is not present in the PBE data, as shown in Fig. 3 (b), and is instead replaced by a much weaker redistribution of charge toward the SiCNT surface. Note that while the D2 and D3 corrections properly address the binding curve, they do not affect the charge density at a given geometry. In contrast, vdW-DF2 and rVV10 achieve their corrections by deforming the charge density (as a side effect of changes at the wavefunction level) using non-local perturbations in the correlation integral. As shown in Fig. 3 (c) and (d) for vdW-DF2 and rVV10, respectively, there is a slight dip in charge density in the shape of a

bow; this is associated with the existence of noncovalent-type interactions [51], although it is much weaker in the rVV10 case. Interestingly, the rVV10 distribution is much closer to the LDA distribution as opposed to the distinct distribution of vdW-DF2. The lack of proper vdW inter-

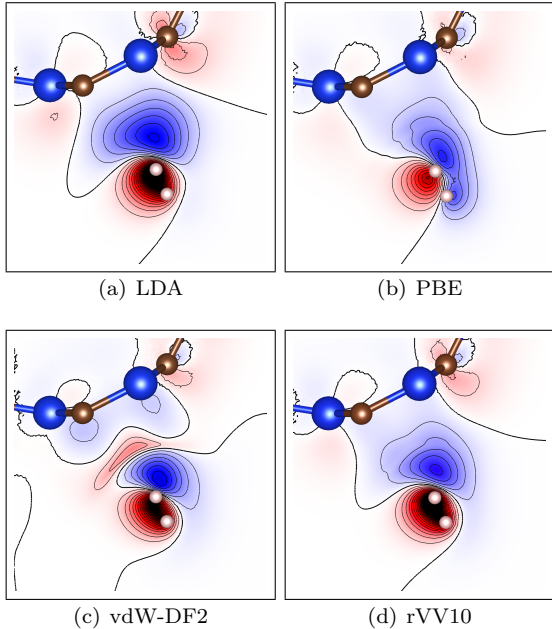


Figure 3: Charge density difference $\Delta\rho(r)$ in the presence of other fragment vs. isolated fragments: (a) LDA, (b) PBE, (c) vdW-DF2, and (d) rVV10. See the text for the definition of $\Delta\rho(r)$. Blue denotes a positive difference, while red denotes a negative difference. The distributions from vdW-DF2 and rVV10 are notably distinct; rVV10 is similar to LDA, while vdW-DF2 shows a slight dip in between despite their similar binding curves.

actions in LDA and GGA results in misestimation by more than 0.5 kcal/mol, with further potential for errors arising from incorrect geometry predictions. Since the target adsorption energy is 3.5–11.5 kcal/mol, this misestimation is not negligible. We thus claim that the inclusion of vdW corrections in the XC functional is essential for the quantitative evaluation of adsorption energies, particularly in the vdW-heavy H_2 -SiCNT system, and more generally for the further computational exploration of storage materials.

3.3. Fully optimized geometries

In Section 3.2, we varied only the distance between H_2 and SiCNT for our benchmark purpose of evaluating the vdW interactions. Here, we consider the fully optimized geometries to evaluate a more realistic adsorption energy. Table 2 gives the structural information obtained from the selected DFT methods. Similar to the findings discussed in Section 3.2, the vdW-corrected functionals clearly give highly similar trends, while LDA (GGA) over (under)-binds. Regarding the vdW-corrected functionals, vdW-DF2 and rVV10 agree well with each other in terms of the structural parameters and adsorption energy. In

particular, the surface angle determined by PBE+D3 is markedly different from those determined by vdW-DF2 and rVV10. The above findings can also be investigated

Table 2: Optimized H_2 conformations and adsorption energies from all tested XC functionals. The energy values are from full optimization calculations.

XC	R_{H_2} [\AA]	θ_s [deg.]	E_{ads} [kcal/mol]
LDA	2.573	51.3	2.375
GGA	3.437	37.6	0.291
PBE+D3	3.000	45.7	1.421
vdW-DF2	3.170	54.4	1.268
rVV10	2.930	53.9	1.298

by the charge density analysis shown in Figure 3. Considering the change in the charge density distribution, LDA and the two vdW-DFT functionals (vdW-DF2 and rVV10) give different shapes than PBE (PBE+D3); the surface angles θ_s for LDA, vdW-DF2, and rVV10 are greater than 50° , whereas PBE and PBE+D3 have smaller θ_s values. Only the pairwise vdW corrections cannot reproduce the structure properly, but the self-consistent charge deformation is also important in obtaining proper structures. As the charge density at the bonding region between H_2 and SiCNT increases (LDA > rVV10 > vdW-DF2), R_{H_2} and θ_s both decrease (LDA < rVV10 < vdW-DF2). As mentioned in Section 3.2, the LDA bonding is not noncovalent but spurious. It is evident from the correlation between the charge density and structure that the LDA overbinding correlates to the highest charge density at the bonding region.

4. Conclusion

We performed DMC calculations and various DFT simulations to evaluate the adsorption energies of a hydrogen molecule on an SiCNT with a (5,5) armchair structure. Recently developed XC functionals designed to reproduce vdW interactions (PBE+D3, vdW-DF2, and rVV10) and conventional XC functionals (LDA-PZ, GGA-PBE, and B3LYP) were compared to DMC as a reference. Overall, all the vdW-corrected XC functionals agree well with DMC, whereas LDA (GGA) over (under)-binds. The self-consistent nonlocal correlation functionals, vdW-DF2 and rVV10, give almost the same adsorption energies. Differences in the structural properties were found to closely correlate with differences in the charge density distribution. A higher charge density in the bonding region leads to a shorter distance between H_2 and SiCNT and larger surface angle. The magnitude of the vdW interaction was estimated to be ca. 51 meV (1.2 kcal/mol), which corresponds to 9–29 % of the ideal adsorption energy for hydrogen storage. This finding implies the importance of vdW corrections within the framework of DFT. We thus

conclude that protocols based on vdW-corrected XC functionals will advance the computational investigation and exploration of storage materials in the near future.

Acknowledgments

The computations in the present study were partially performed using the facilities of the Research Center for Advanced Computing Infrastructure (RCACI) at JAIST and resources of the Argonne Leadership Computing Facility, which is a DOE Office of Science User Facility supported under Contract No. DE-AC02-06CH11357 through an award provided by the Innovative and Novel Computational Impact on Theory and Experiment (INCITE) program. A.B. and H.S. were supported by the U.S. Department of Energy, Office of Science, Basic Energy Sciences, Materials Sciences and Engineering Division, as part of the Computational Materials Sciences Program and Center for Predictive Simulation of Functional Materials. R.M. is grateful for financial supports from MEXT-KAKENHI (JP19H04692 and JP16KK0097), FLAGSHIP2020 (project nos. hp190169 and hp190167 at K-computer), the Air Force Office of Scientific Research (AFOSR-AOARD/FA2386-17-1-4049; FA2386-19-1-4015), and JSPS Bilateral Joint Projects (with India DST). K.H. is grateful for financial support from the HPCI System Research Project (Project ID: hp190169) and MEXT-KAKENHI (JP16H06439, JP17K17762, JP19K05029, and JP19H05169).

References

- [1] I. Dincer, Technical, environmental and exergetic aspects of hydrogen energy systems, *International Journal of Hydrogen Energy* 27 (3) (2002) 265–285. doi:[https://doi.org/10.1016/S0360-3199\(01\)00119-7](https://doi.org/10.1016/S0360-3199(01)00119-7). URL <https://www.sciencedirect.com/science/article/pii/S0360319901001197>
- [2] U. Eberle, M. Felderhoff, F. Schüth, Chemical and Physical Solutions for Hydrogen Storage, *Angewandte Chemie International Edition* 48 (36) (2009) 6608–6630. doi:[10.1002/anie.200806293](https://doi.org/10.1002/anie.200806293). URL <http://doi.wiley.com/10.1002/anie.200806293>
- [3] O. Gröger, H. A. Gasteiger, J.-P. Suchsland, Review—electromobility: Batteries or fuel cells?, *Journal of The Electrochemical Society* 162 (14) (2015) A2605–A2622. doi:[10.1149/2.0211514jes](https://doi.org/10.1149/2.0211514jes). URL <https://doi.org/10.1149/2.0211514jes>
- [4] S.-H. Jhi, Activated boron nitride nanotubes: A potential material for room-temperature hydrogen storage, *Physical Review B* 74 (15) (Oct. 2006). doi:[10.1103/PhysRevB.74.155424](https://doi.org/10.1103/PhysRevB.74.155424). URL <https://link.aps.org/doi/10.1103/PhysRevB.74.155424>
- [5] S. K. Bhatia, A. L. Myers, Optimum conditions for adsorptive storage, *Langmuir* 22 (4) (2006) 1688–1700, PMID: 16460092. arXiv:<https://doi.org/10.1021/la0523816>, doi:[10.1021/la0523816](https://doi.org/10.1021/la0523816). URL <https://doi.org/10.1021/la0523816>
- [6] G. Mpourmpakis, G. E. Froudakis, George P. Lithoxoos, J. Samios, SiC Nanotubes: A Novel Material for Hydrogen Storage, *Nano Letters* 6 (8) (2006) 1581–1583. doi:[10.1021/nl0603911](https://doi.org/10.1021/nl0603911). URL <http://pubs.acs.org/doi/abs/10.1021/nl0603911>
- [7] N. R. Devi, V. Gayathri, Effect of structural defects on the hydrogen adsorption in promising nanostructures, *Computational Materials Science* 96 (2015) 284–289. doi:[10.1016/j.commatsci.2014.09.017](https://doi.org/10.1016/j.commatsci.2014.09.017). URL <http://www.sciencedirect.com/science/article/pii/S0927025614006284>
- [8] C. Tabtimsai, V. Ruangpornvisuti, S. Tontapha, B. Wannoo, A DFT investigation on group 8b transition metal-doped silicon carbide nanotubes for hydrogen storage application, *Applied Surface Science* 439 (2018) 494–505. doi:[10.1016/j.apsusc.2017.12.255](https://doi.org/10.1016/j.apsusc.2017.12.255). URL <https://linkinghub.elsevier.com/retrieve/pii/S0169433217339156>
- [9] X. Wang, K. M. Liew, Hydrogen Storage in Silicon Carbide Nanotubes by Lithium Doping, *The Journal of Physical Chemistry C* 115 (8) (2011) 3491–3496. doi:[10.1021/jp106509g](https://doi.org/10.1021/jp106509g). URL <http://pubs.acs.org/doi/10.1021/jp106509g>
- [10] A. Mavrandonakis, G. E. Froudakis, M. Schnell, M. Mühlhäuser, From Pure Carbon to Silicon-Carbon Nanotubes: An Ab-initio Study, *Nano Letters* 3 (11) (2003) 1481–1484. doi:[10.1021/nl0343250](https://doi.org/10.1021/nl0343250). URL <http://pubs.acs.org/doi/abs/10.1021/nl0343250>
- [11] K. M. Alam, A. K. Ray, A hybrid density functional study of zigzag SiC nanotubes, *Nanotechnology* 18 (49) (2007) 495706. doi:[10.1088/0957-4484/18/49/495706](https://doi.org/10.1088/0957-4484/18/49/495706). URL <http://stacks.iop.org/0957-4484/18/i=49/a=495706?key=crossref.2fcffaf9a6d02c7a2bea5f99c8dbc8db>
- [12] B. Baumeier, P. Krüger, J. Pollmann, Structural, elastic, and electronic properties of SiC, BN, and BeO nanotubes, *Physical Review B* 76 (8) (Aug. 2007). doi:[10.1103/PhysRevB.76.085407](https://doi.org/10.1103/PhysRevB.76.085407). URL <https://link.aps.org/doi/10.1103/PhysRevB.76.085407>
- [13] S. H. Barghi, T. T. Tsotsis, M. Sahimi, Chemisorption, physisorption and hysteresis during hydrogen storage in carbon nanotubes, *International Journal of Hydrogen Energy* 39 (3) (2014) 1390–1397. doi:[10.1016/j.ijhydene.2013.10.163](https://doi.org/10.1016/j.ijhydene.2013.10.163). URL <https://linkinghub.elsevier.com/retrieve/pii/S0360319913026785>
- [14] S. Banerjee, S. Nigam, C. Pillai, C. Majumder, Hydrogen storage on ti decorated sic nanostructures: A first principles study, *International Journal of Hydrogen Energy* 37 (4) (2012) 3733 – 3740, international Conference on Renewable Energy (ICRE 2011). doi:<https://doi.org/10.1016/j.ijhydene.2011.05.078>. URL <http://www.sciencedirect.com/science/article/pii/S0360319911012900>
- [15] R. J. Baierle, R. H. Miwa, Hydrogen interaction with native defects in SiC nanotubes, *Physical Review B* 76 (20) (2007) 205410. doi:[10.1103/PhysRevB.76.205410](https://doi.org/10.1103/PhysRevB.76.205410). URL <https://link.aps.org/doi/10.1103/PhysRevB.76.205410>
- [16] X. W. Sheng, L. Mentel, O. V. Gritsenko, E. J. Baerends, Counterpoise correction is not useful for short and van der waals distances but may be useful at long range, *Journal of Computational Chemistry* 32 (13) (2011) 2896–2901. arXiv:<https://onlinelibrary.wiley.com/doi/pdf/10.1002/jcc.21872>, doi:<https://doi.org/10.1002/jcc.21872>. URL <https://onlinelibrary.wiley.com/doi/abs/10.1002/jcc.21872>
- [17] S. H. Barghi, T. T. Tsotsis, M. Sahimi, Hydrogen sorption hysteresis and superior storage capacity of silicon-carbide nanotubes over their carbon counterparts, *International Journal of Hydrogen Energy* 39 (36) (2014) 21107–21115. doi:[10.1016/j.ijhydene.2014.10.087](https://doi.org/10.1016/j.ijhydene.2014.10.087). URL <http://www.sciencedirect.com/science/article/pii/S0360319914029279>
- [18] S. H. Barghi, T. T. Tsotsis, M. Sahimi, Experimental investigation of hydrogen adsorption in doped silicon-carbide nanotubes, *International Journal of Hydrogen Energy* 41 (1) (2016) 369–374. doi:[10.1016/j.ijhydene.2015.10.091](https://doi.org/10.1016/j.ijhydene.2015.10.091)

- URL <http://linkinghub.elsevier.com/retrieve/pii/S0360319915025884>
- [19] M. Korth, A. Luchow, S. Grimme, Toward the exact solution of the electronic schrodinger equation for noncovalent molecular interactions: Worldwide distributed quantum monte carlo calculations, *The Journal of Physical Chemistry A* 112 (10) (2008) 2104–2109. arXiv:<http://pubs.acs.org/doi/pdf/10.1021/jp077592t>, doi:10.1021/jp077592t. URL <http://pubs.acs.org/doi/abs/10.1021/jp077592t>
- [20] K. Hongo, M. A. Watson, R. S. Sánchez-Carrera, T. Iitaka, A. Aspuru-Guzik, Failure of conventional density functionals for the prediction of molecular crystal polymorphism: A quantum monte carlo study, *J. Phys. Chem. Lett.* 1 (12) (2010) 1789–1794. arXiv:<https://doi.org/10.1021/jz100418p>, doi:10.1021/jz100418p. URL <https://doi.org/10.1021/jz100418p>
- [21] M. A. Watson, K. Hongo, T. Iitaka, A. Aspuru-Guzik, A Benchmark Quantum Monte Carlo Study of Molecular Crystal Polymorphism: A Challenging Case for Density-Functional Theory, Ch. 9, pp. 101–117. arXiv:<https://pubs.acs.org/doi/pdf/10.1021/bk-2012-1094.ch009>, doi:10.1021/bk-2012-1094.ch009. URL <https://pubs.acs.org/doi/abs/10.1021/bk-2012-1094.ch009>
- [22] M. Dubecký, P. Jurečka, R. Derian, P. Hobza, M. Otyepka, L. Mitas, Quantum monte carlo methods describe noncovalent interactions with subchemical accuracy, *Journal of Chemical Theory and Computation* 9 (10) (2013) 4287–4292. arXiv:<http://pubs.acs.org/doi/pdf/10.1021/ct4006739>, doi:10.1021/ct4006739. URL <http://pubs.acs.org/doi/abs/10.1021/ct4006739>
- [23] M. Dubecký, R. Derian, P. Jurečka, L. Mitas, P. Hobza, M. Otyepka, Quantum monte carlo for noncovalent interactions: an efficient protocol attaining benchmark accuracy, *Phys. Chem. Chem. Phys.* 16 (2014) 20915–20923. doi:10.1039/C4CP02093F. URL <http://dx.doi.org/10.1039/C4CP02093F>
- [24] K. Hongo, N. T. Cuong, R. Maezono, The importance of electron correlation on stacking interaction of adenine-thymine base-pair step in B-DNA: A quantum Monte Carlo study, *J. Chem. Theory Comput.* 9 (2) (2013) 1081–1086. doi:10.1021/ct301065f.
- [25] K. Hongo, M. A. Watson, T. Iitaka, A. Aspuru-Guzik, R. Maezono, Diffusion monte carlo study of para-diiodobenzene polymorphism revisited, *J. Chem. Theory Comput.* 11 (3) (2015) 907–917, pMID: 26579744. arXiv:<https://doi.org/10.1021/ct500401p>, doi:10.1021/ct500401p. URL <https://doi.org/10.1021/ct500401p>
- [26] K. Hongo, R. Maezono, Practical Diffusion Monte Carlo Simulations for Large Noncovalent Systems, Ch. 9, pp. 127–143. arXiv:<https://pubs.acs.org/doi/pdf/10.1021/bk-2016-1234.ch009>, doi:10.1021/bk-2016-1234.ch009. URL <https://pubs.acs.org/doi/abs/10.1021/bk-2016-1234.ch009>
- [27] M. Dubecký, L. Mitas, P. Jurečka, Noncovalent Interactions by Quantum Monte Carlo, *Chemical Reviews* 116 (9) (2016) 5188–5215. doi:10.1021/acs.chemrev.5b00577. URL <http://pubs.acs.org/doi/10.1021/acs.chemrev.5b00577>
- [28] K. Hongo, R. Maezono, A computational scheme to evaluate hamaker constants of molecules with practical size and anisotropy, *J. Chem. Theory Comput.* 13 (11) (2017) 5217–5230, pMID: 28981266. arXiv:<https://doi.org/10.1021/acs.jctc.6b01159>, doi:10.1021/acs.jctc.6b01159. URL <https://doi.org/10.1021/acs.jctc.6b01159>
- [29] K. Oqmhula, K. Hongo, R. Maezono, T. Ichibha, Ab initio evaluation of complexation energies for cyclodextrin-drug inclusion complexes, *ACS Omega* 5 (31) (2020) 19371–19376. arXiv:<https://doi.org/10.1021/acsomega.0c01059>, doi:10.1021/acsomega.0c01059. URL <https://doi.org/10.1021/acsomega.0c01059>
- [30] K. M. Alam, A. K. Ray, Hybrid density functional study of armchair SiC nanotubes, *Physical Review B* 77 (3) (Jan. 2008). doi:10.1103/PhysRevB.77.035436. URL <https://link.aps.org/doi/10.1103/PhysRevB.77.035436>
- [31] M. Menon, E. Richter, A. Mavrandonakis, G. Froudakis, A. N. Andriotis, Structure and stability of SiC nanotubes, *Physical Review B* 69 (11) (Mar. 2004). doi:10.1103/PhysRevB.69.115322. URL <https://link.aps.org/doi/10.1103/PhysRevB.69.115322>
- [32] J. T. Frey, D. J. Doren, Tubegen 3.4, <http://turin.nss.udel.edu/research/tubegenonline.html> (2011).
- [33] P. Giannozzi, S. Baroni, N. Bonini, M. Calandra, R. Car, C. Cavazzoni, D. Ceresoli, G. L. Chiarotti, M. Cococcioni, I. Dabo, A. D. Corso, S. de Gironcoli, S. Fabris, G. Fratesi, R. Gebauer, U. Gerstmann, C. Gougoussis, A. Kokalj, M. Lazzeri, L. Martin-Samos, N. Marzari, F. Mauri, R. Mazzarello, S. Paolini, A. Pasquarello, L. Paulatto, C. Sbraccia, S. Scandolo, G. Sclauzero, A. P. Seitsonen, A. Smogunov, P. Umari, R. M. Wentzcovitch, Quantum espresso: a modular and open-source software project for quantum simulations of materials, *Journal of Physics: Condensed Matter* 21 (39) (2009) 395502. URL <http://stacks.iop.org/0953-8984/21/i=39/a=395502>
- [34] H. J. Monkhorst, J. D. Pack, Special points for brillouin-zone integrations, *Physical Review B* 13 (1976) 5188–5192. doi:10.1103/PhysRevB.13.5188. URL <https://link.aps.org/doi/10.1103/PhysRevB.13.5188>
- [35] M. Burkatzki, C. Filippi, M. Dolg, Energy-consistent pseudopotentials for quantum monte carlo calculations, *The Journal of Chemical Physics* 126 (23) (2007) 234105. arXiv:<https://doi.org/10.1063/1.2741534>, doi:10.1063/1.2741534. URL <https://doi.org/10.1063/1.2741534>
- [36] M. Dion, H. Rydberg, E. Schröder, D. C. Langreth, B. I. Lundqvist, Van der waals density functional for general geometries, *Physical Review Letters* 92 (2004) 246401. doi:10.1103/PhysRevLett.92.246401. URL <https://link.aps.org/doi/10.1103/PhysRevLett.92.246401>
- [37] S. Grimme, Semiempirical gga-type density functional constructed with a long-range dispersion correction, *Journal of Computational Chemistry* 27 (15) (2006) 1787–1799. arXiv:<https://onlinelibrary.wiley.com/doi/pdf/10.1002/jcc.20495>, doi:10.1002/jcc.20495. URL <https://onlinelibrary.wiley.com/doi/abs/10.1002/jcc.20495>
- [38] S. Grimme, J. Antony, S. Ehrlich, H. Krieg, A consistent and accurate ab initio parametrization of density functional dispersion correction (dft-d) for the 94 elements h-pu, *The Journal of Chemical Physics* 132 (15) (2010) 154104. arXiv:<https://doi.org/10.1063/1.3382344>, doi:10.1063/1.3382344. URL <https://doi.org/10.1063/1.3382344>
- [39] K. Lee, E. D. Murray, L. Kong, B. I. Lundqvist, D. C. Langreth, Higher-accuracy van der waals density functional, *Physical Review B* 82 (2010) 081101. doi:10.1103/PhysRevB.82.081101. URL <https://link.aps.org/doi/10.1103/PhysRevB.82.081101>
- [40] R. Sabatini, T. Gorni, S. de Gironcoli, Nonlocal van der waals density functional made simple and efficient, *Physical Review B* 87 (2013) 041108. doi:10.1103/PhysRevB.87.041108. URL <https://link.aps.org/doi/10.1103/PhysRevB.87.041108>
- [41] T. Thonhauser, S. Zuluaga, C. A. Arter, K. Berland, E. Schröder, P. Hyldgaard, Spin signature of nonlocal correlation binding in metal-organic frameworks, *Physical Review Letters* 115 (2015) 136402. doi:10.1103/PhysRevLett.115.136402. URL <https://link.aps.org/doi/10.1103/PhysRevLett.115.136402>
- [42] J. P. Perdew, A. Zunger, Self-interaction correction to density-functional approximations for many-electron systems, *Physical*

- Review B 23 (1981) 5048–5079. doi:10.1103/PhysRevB.23.5048.
 URL <https://link.aps.org/doi/10.1103/PhysRevB.23.5048>
- [43] J. P. Perdew, K. Burke, M. Ernzerhof, Generalized gradient approximation made simple, *Physical Review Letters* 77 (1996) 3865–3868. doi:10.1103/PhysRevLett.77.3865.
 URL <https://link.aps.org/doi/10.1103/PhysRevLett.77.3865>
- [44] J. Kim, A. D. Baczewski, T. D. Beaudet, A. Benali, M. C. Bennett, M. A. Berrill, N. S. Blunt, E. J. L. Borda, M. Casula, D. M. Ceperley, S. Chiesa, B. K. Clark, R. C. Clay, K. T. Delaney, M. Dewing, K. P. Esler, H. Hao, O. Heinonen, P. R. C. Kent, J. T. Krogel, I. Kylänpää, Y. W. Li, M. G. Lopez, Y. Luo, F. D. Malone, R. M. Martin, A. Mathuriya, J. McMinis, C. A. Melton, L. Mitas, M. A. Morales, E. Neuscamman, W. D. Parker, S. D. P. Flores, N. A. Romero, B. M. Rubenstein, J. A. R. Shea, H. Shin, L. Shulenburger, A. F. Tillack, J. P. Townsend, N. M. Tubman, B. V. D. Goetz, J. E. Vincent, D. C. Yang, Y. Yang, S. Zhang, L. Zhao, QMCPACK: an open source ab initio quantum monte carlo package for the electronic structure of atoms, molecules and solids, *Journal of Physics: Condensed Matter* 30 (19) (2018) 195901. doi:10.1088/1361-648x/aab9c3.
 URL <https://doi.org/10.1088/1361-648x/aab9c3>
- [45] J. Toulouse, C. J. Umrigar, Optimization of quantum monte carlo wave functions by energy minimization, *The Journal of Chemical Physics* 126 (8) (2007) 084102. arXiv:<https://doi.org/10.1063/1.2437215>, doi:10.1063/1.2437215.
 URL <https://doi.org/10.1063/1.2437215>
- [46] L. Otis, E. Neuscamman, Complementary first and second derivative methods for ansatz optimization in variational monte carlo, *Phys. Chem. Chem. Phys.* 21 (2019) 14491–14510. doi:10.1039/C9CP02269D.
 URL <http://dx.doi.org/10.1039/C9CP02269D>
- [47] D. Alfè, M. J. Gillan, Efficient localized basis set for quantum Monte Carlo calculations on condensed matter, *Physical Review B* 70 (16) (2004) 161101. doi:10.1103/PhysRevB.70.161101.
 URL <https://link.aps.org/doi/10.1103/PhysRevB.70.161101>
- [48] M. Casula, S. Moroni, S. Sorella, C. Filippi, Size-consistent variational approaches to nonlocal pseudopotentials: Standard and lattice regularized diffusion monte carlo methods revisited, *The Journal of Chemical Physics* 132 (15) (2010) 154113. arXiv:<https://doi.org/10.1063/1.3380831>, doi:10.1063/1.3380831.
 URL <https://doi.org/10.1063/1.3380831>
- [49] C. Lin, F. H. Zong, D. M. Ceperley, Twist-averaged boundary conditions in continuum quantum monte carlo algorithms, *Phys. Rev. E* 64 (2001) 016702. doi:10.1103/PhysRevE.64.016702.
 URL <https://link.aps.org/doi/10.1103/PhysRevE.64.016702>
- [50] Y. Wang, C. Zhao, K. Su, X. Wang, X. Qin, Z. Yuan, A Density Functional Theoretical Study on Ultra Long Armchair (n, n) Single Walled Carbon Silicon Nanotubes, *Journal of Nanoscience and Nanotechnology* 17 (6) (2017) 3809–3815. doi:10.1166/jnn.2017.13995.
 URL <http://www.ingentaconnect.com/content/10.1166/jnn.2017.13995>
- [51] J. Contreras-García, E. R. Johnson, S. Keinan, R. Chaudret, J.-P. Piquemal, D. N. Beratan, W. Yang, Nciplot: A program for plotting noncovalent interaction regions, *Journal of Chemical Theory and Computation* 7 (3) (2011) 625–632, pMID: 21516178. arXiv:<https://doi.org/10.1021/ct100641a>, doi:10.1021/ct100641a.
 URL <https://doi.org/10.1021/ct100641a>